TISSUE ENGINEERING
Volume 9, Number 2, 2003

Analytical Model for Predicting Mechanotransduction Effects in Engineered Cardiac Tissue

DAVID C. LATIMER, D.Phil.,[1] BRADLEY J. ROTH, Ph.D.,[2] and KEVIN KIT PARKER, Ph.D.[3]

ABSTRACT

Mechanochemical and mechanoelectrical signaling is imperative for cardiac organogenesis and underlies pathophysiological events. New techniques for engineering cardiac tissue allow unprecedented means of modeling these phenomena *in vitro*. However, experimental design is often hampered by a lack of models that can be adapted to the ideal conditions these methods allow. To address these deficiencies, we developed a mathematical model to calculate the distribution of stress and strain in fibrous cardiac tissue. The fluid–fiber–collagen model characterizes the mechanical behavior of cardiac tissue and is solved analytically for the distributions of stress and strain along the myocardial fibers. An example application of the model is presented: modeling the distribution of strains in the vicinity of an ischemic region. The ischemic region is stretched during systole, as has been shown in previous one-dimensional models. Our model predicts a complex distribution of stretch in the border zone surrounding the ischemic region and in nonischemic regions surrounding the border zone. These strain patterns may predict patterns of mechanochemical coupling that results in localized fibrosis, altered gene expression, or the mechanoelectrical signaling events that potentiate cardiac arrhythmias.

INTRODUCTION

Stresses and strains within tissue have been found to potentiate a variety of cellular effects, from tissue development to terminal disease.[1–3] Nowhere is the role of mechanotransduction more complex than in cardiac muscle, where both physiological and pathological remodeling of the tissue, as well as fatal arrhythmias, have been attributed to mechanical forces.[4–6] The geometric complexity of the heart and the unique dynamics of the cardiac tissue microenvironment have made it difficult to elucidate the mechanochemical and mechanoelectrical signaling pathways that underlie these events. Mechanical stress-induced hypertrophy and remodeling after myocardial infarction are examples of such processes, where wall stress and strain patterns potentiate altered gene expression patterns, resulting in fibrosis, misalignment of sarcomeres, altered cytoskeletal architecture, and an increased incidence of cardiac arrhythmias.[7–9] New techniques[10–12] for modeling the tissue microenvironment provide unique opportunities for studying cardiac tissue in two- and three-dimensional preparations.[13–15] However, experimental strategies are often hampered by a lack of generalized, analytical models that will allow the experimentalist to apply fundamental engineering design principles. This is especially true in modeling cardiac mechanics, where most models are highly constrained in an effort to model *in vivo* histology and require numerical techniques to solve.[16,17]

These circumstances prompted us to ask: can we de-

[1]Department of Physics and Astronomy, Vanderbilt University, Nashville, Tennessee.
[2]Department of Physics, Oakland University, Rochester, Michigan.
[3]Whitaker Biomedical Engineering Institute, Johns Hopkins School of Medicine, Baltimore, Maryland.

velop an analytical model of the stress and strain distributions in cardiac tissue? We adapted a previous model[18] to two- and three-dimensional idealized cardiac tissues and derived an analytical solution to the stress and strain in the tissue. When the model is applied to the strain distribution in or near an infarcted zone, a complex distribution of strain gradients is calculated, not only in the ischemic border zone, but also in areas at a distance from the infarct itself. These results are similar to magnetic resonance imaging (MRI) tagging experiments, where tissue deformation was observed in outlying regions from the infarcted zone. These variations in the spatial distribution of strain may underlie the remodeling that is observed clinically after myocardial infarction. It is hoped that the mathematical model presented here will aid the design of engineered models of the cardiac tissue microenvironment.

METHODS

Two-dimensional model

We assume that the myocardial fibers align with the x axis, and we use a polar coordinate system to specify position (r, θ). The continuum fluid–fiber–collagen model[18] represents the mechanical properties of the tissue. The stress tensor, σ_{ij}, is

$$\sigma_{ij} = -p\delta_{ij} + T\tau_i\tau_j + 2\mu\epsilon_{ij} \tag{1}$$

where p is the myocardial tissue pressure, δ_{ij} is the Kronecker delta, T is the tension of the myocardial fibers, τ is a unit vector parallel to the local fiber direction, μ is the shear modulus, and ϵ_{ij} is the strain tensor. The first term in Eq. (1) accounts for the fluid hydrostatic pressure plus a contribution from the incompressible collagen strut matrix. The second term represents the active tension developed by the myocardium, acting in the direction parallel to the myocardial fibers. In polar coordinates, this term becomes

$$T\tau_i\tau_j = T \begin{bmatrix} \cos^2\theta & -\cos\theta\sin\theta \\ -\cos\theta\sin\theta & \sin^2\theta \end{bmatrix} \tag{2}$$

with T assumed to be independent of strain. The third term characterizes the strain within the extracellular collagen matrix. We assume that the collagen matrix is isotropic, and that the strains are small enough that we can use a linear model for the strain tensor.

The equations of quasistatic mechanical equilibrium in polar coordinates are[19]

$$\frac{\partial\sigma_{rr}}{\partial r} + \frac{1}{r}\frac{\partial\sigma_{r\theta}}{\partial\theta} + \frac{\sigma_{rr} - \sigma_{\theta\theta}}{r} = 0 \tag{3a}$$

$$\frac{\partial\sigma_{r\theta}}{\partial r} + \frac{1}{r}\frac{\partial\sigma_{\theta\theta}}{\partial\theta} + \frac{2\,\sigma_{r\theta}}{r} = 0 \tag{3b}$$

The displacement of the tissue $\mathbf{u} = (u_r, u_\theta)$ determines the strain tensor. In polar coordinates,[19]

$$\epsilon_{rr} = \frac{\partial u_r}{\partial r} \qquad \epsilon_{\theta\theta} = \frac{u_r}{r} + \frac{1}{r}\frac{\partial u_\theta}{\partial\theta}$$
$$\epsilon_{r\theta} = \frac{1}{2}\left(\frac{1}{r}\frac{\partial u_r}{\partial\theta} + \frac{\partial u_\theta}{\partial r} - \frac{u_\theta}{r}\right) \tag{4a–c}$$

We assume that the tissue is incompressible ($\nabla\cdot u = 0$). Incompressibility implies the displacement can be specified by a stream function ψ,

$$u_r = -\frac{1}{r}\frac{\partial\psi}{\partial\theta} \qquad u_\theta = \frac{\partial\psi}{\partial r} \tag{5a and b}$$

We model an inhomogeneous (ischemic) region as a circle of radius a (Fig. 1). The ischemic tissue represents an inhomogeneity that is unable to generate an active stress during systole ($T = 0$, $r <$ a; $T = T_o$, $r > a$). At the border of this inhomogeneous region ($r = a$), the displacement and the radial components of the stress tensor are continuous. As r approaches infinity, the displacement approaches zero (fixed boundary). The solution is unique, except for a constant, uniform pressure term.[20]

Three-dimensional model

The three-dimensional model is analogous to the two-dimensional model. We assume that the fibers align with the z axis, and we use a spherical coordinate system (r, θ, ϕ). The stress and strain are independent of the angle ϕ (azimuthal symmetry). The stress tensor is given by Eq. (1). In spherical coordinates, the second term of Eq. (1) becomes

$$T\tau_i\tau_j = \frac{T}{2}\begin{bmatrix} \cos2\theta + 1 & -\sin2\theta & 0 \\ -\sin2\theta & \cos2\theta - 1 & 0 \\ 0 & 0 & 0 \end{bmatrix} \tag{6}$$

The equations of quasistatic mechanical equilibrium in spherical coordinates are[19]

$$\frac{\partial\sigma_{rr}}{\partial r} + \frac{1}{r}\frac{\partial\sigma_{r\theta}}{\partial\theta} + \frac{1}{r\sin\theta}\frac{\partial\sigma_{r\phi}}{\partial\phi} + \frac{1}{r}(2\sigma_{rr} - \sigma_{\theta\theta} - \sigma_{r\phi} - \sigma_{r\theta}\cot\theta) = 0 \tag{7a}$$

$$\frac{\partial\sigma_{r\theta}}{\partial r} + \frac{1}{r}\frac{\partial\sigma_{\theta\theta}}{\partial\theta} + \frac{1}{r\sin\theta}\frac{\partial\sigma_{\theta\phi}}{\partial\phi} + \frac{1}{r}[(\sigma_{\theta\theta} - \sigma_{\phi\phi})\cot\theta + 3\sigma_{r\theta}] = 0 \tag{7b}$$

$$\frac{\partial\sigma_{r\phi}}{\partial r} + \frac{1}{r}\frac{\partial\sigma_{\theta\phi}}{\partial\theta} + \frac{1}{r\sin\theta}\frac{\partial\sigma_{\phi\phi}}{\partial\phi} + \frac{1}{r}(3\sigma_{r\phi} + 2\sigma_{\theta\phi}\cot\theta) = 0 \tag{7c}$$

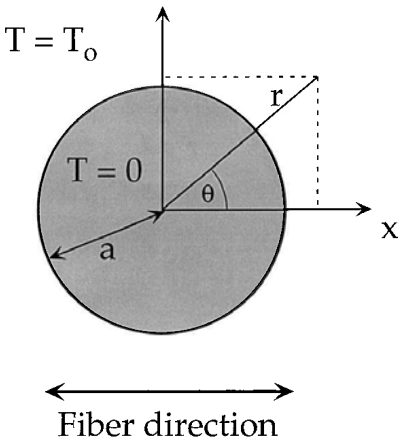

FIG. 1. Schematic diagram of tissue geometry.

The displacement $\mathbf{u} = (u_r, u_\theta, u_\phi)$ determines the strain tensor. In spherical coordinates,[19]

$$\epsilon_{rr} = \frac{\partial u_r}{\partial r} \qquad \epsilon_{\theta\theta} = \frac{1}{r}\frac{\partial u_\theta}{\partial \theta} + \frac{u_r}{r} \tag{8a and b}$$

$$\epsilon_{\phi\phi} = \frac{1}{r \sin\theta}\frac{\partial u_\phi}{\partial \phi} + \frac{u_\theta}{r}\cot\theta + \frac{u_r}{r}$$

$$\epsilon_{r\theta} = \frac{1}{2}\left(\frac{\partial u_\theta}{\partial r} - \frac{u_\theta}{r} + \frac{1}{r}\frac{\partial u_r}{\partial \theta}\right) \tag{8c and d}$$

$$\epsilon_{\theta\phi} = \frac{1}{2r}\left(\frac{\partial u_\phi}{\partial \theta} - u_\phi \cot\theta + \frac{1}{\sin\theta}\frac{\partial u_\theta}{\partial \phi}\right) \tag{8e}$$

$$\epsilon_{\phi r} = \frac{1}{2}\left(\frac{1}{r \sin\theta}\frac{\partial u_r}{\partial \phi} + \frac{\partial u_\phi}{\partial r} - \frac{u_\phi}{r}\right) \tag{8f}$$

Incompressibility and azimuthal symmetry imply the displacement can be specified by a stream function ψ,

$$u_r = \frac{1}{r^2 \sin\theta}\frac{\partial \psi}{\partial \theta} \qquad u_\theta = -\frac{1}{r \sin\theta}\frac{\partial \psi}{\partial r} \tag{9a and b}$$

We model an ischemic region as a sphere of radius a ($T = 0$, $r < a$; $T = T_o$, $r >$ a).

RESULTS

Two-dimensional model

We must determine ψ and p in the inner (i, $r < a$) and outer (o, $r > a$) regions, subject to Eqs. (1)–(5) along with the boundary conditions. The solution can be found analytically, and is

$$\psi_i = -\left(\frac{T_o}{8\mu}\right)\frac{r^2}{2}\sin 2\theta \tag{10}$$

$$p_i = -\frac{T_o}{2} \tag{11}$$

$$\psi_o = -\left(\frac{T_o}{8\mu}\right)a^2\left[1 - \frac{1}{2}\left(\frac{a}{r}\right)^2\right]\sin 2\theta \tag{12}$$

$$p_o = \frac{T_o}{2}\left(\frac{a}{r}\right)^2 \cos 2\theta \tag{13}$$

All components of the stress and strain tensors can be calculated from ψ and p, using Eqs. (1)–(5).

The model can be used to predict directionally biased mechanotransduction events. For example, Sachs[21] has modeled stretch-activated channels as having a conductance that depends on the strain parallel to the fibers, ϵ_{xx} (i.e., sarcomere length). We can write ϵ_{xx} in terms of the strain tensor in polar coordinates as $\epsilon_{xx} = \epsilon_{rr}\cos^2\theta + \epsilon_{\theta\theta}\sin^2\theta - \epsilon_{r\theta}2\cos\theta\sin\theta$. In our model, the strain parallel to the muscle fibers is

$$\epsilon_{xx} = \frac{T_o}{8\mu} \quad (r < a) \tag{14a}$$

$$\epsilon_{xx} = \frac{T_o}{8\mu}\left[-2\left(\frac{a}{r}\right)^2 + 3\left(\frac{a}{r}\right)^4\right]\cos 4\theta \quad (r > a) \tag{14b}$$

Figure 2a contains a plot of ϵ_{xx}. The ischemic region stretches uniformly (yellow), and regions in the ischemic border zone surrounding the inhomogeneity stretch in a complex pattern (red and blue). The magnitudes of stretch along the fiber length may be used to predict the opening of stretch-activated ion channels and the initiation of action potential propagation potentiated by their opening.

Three-dimensional model

In three dimensions, the solution is

$$\psi_i = \frac{T_o}{30\mu} r^3 \sin\theta \sin 2\theta \tag{15}$$

$$p_i = 0 \tag{16}$$

$$\psi_o = \frac{T_o}{12\mu} a^3\left[1 - \frac{3}{5}\left(\frac{a}{r}\right)^2\right]\sin\theta \sin 2\theta \tag{17}$$

$$p_o = \frac{T_o}{3}\left[1 + \frac{1}{2}\left(\frac{a}{r}\right)^3 (3\cos 2\theta + 1)\right] \tag{18}$$

and

$$\epsilon_{zz} = \frac{2T_o}{15\mu} \tag{19a}$$

$$\epsilon_{zz} = -\frac{5}{48}\frac{T_o}{\mu}\left\{\left[\left(\frac{a}{r}\right)^3 - \frac{27}{25}\left(\frac{a}{r}\right)^5\right] + \frac{12}{5}\left[\left(\frac{a}{r}\right)^3 - \left(\frac{a}{r}\right)^5\right]\cos 2\theta + \frac{3}{5}\left[5\left(\frac{a}{r}\right)^3 - 7\left(\frac{a}{r}\right)^5\right]\cos 4\theta\right\} \quad (r > a) \tag{19b}$$

Figure 2b contains a plot of ϵ_{zz}. The result is qualitatively similar to the results of the two-dimensional model, except that the stretch along the z axis (the poles of the sphere) is greater than the stretch along the x and y axes

(the equator). Figure 3 shows the full three-dimensional distribution of ϵ_{zz}.

DISCUSSION

We have developed a model for calculating stress and strain in two- and three-dimensional engineered cardiac tissue. Furthermore, we have calculated analytically the stress and strain distribution around an inhomogeneous region in cardiac tissue, with the goal of understanding the mechanical strain of cardiac tissue near an idealized ischemic region. We demonstrate that there can be a complex distribution of strain in the ischemic border zone surrounding the inhomogeneous region. We speculate that the distribution of strains in the tissue volume may explain eccentric patterns of aberrant gene expression, fibrosis, and electrical wave propagation in the remodeled tissue.

Our mathematical calculation is based on the fluid–fiber–collagen model of cardiac tissue.[18,22,23] In our calculation, we make several assumptions:

1. Strains are small enough for a linear model of elasticity.
2. Mechanical properties of the collagen matrix are isotropic.
3. Tissue is in quasistatic mechanical equilibrium.
4. Active tension is independent of strain.
5. Myocardial fibers are straight and are all parallel to one another (no rotation of the fiber direction with depth).
6. The inhomogeneous region is circular or spherical, with a sharp border separating normal and abnormal tissue.
7. The tissue is incompressible.
8. The effects of ischemia on the mechanical properties of cardiac tissue can be accounted for by setting the active tension to zero.
9. The tissue is unbounded.
10. The boundary far from the inhomogeneity is fixed.

While some of the assumptions are probably accurate (e.g., quasistatic mechanical equilibrium, incompressible tissue), others are questionable. In the original formulation of the fluid–fiber–collagen model,[18,22] active tension depends on the tissue strain because of changes in the degree of overlap between the actin and myosin fibers responsible for contraction. This well-known behavior is thought to be the basis for the Frank–Starling mechanism in the heart. The effect is absent in our model. The elastic properties of the collagen may be anisotropic, and during chronic ischemia they may be different in normal and abnormal tissue. Our model for engineered cardiac tissue treats the collagen as isotropic, so we can use a single parameter—the shear modulus μ—to characterize its mechanical properties. Also, we assume that the mechanical properties of collagen are uniform throughout the tissue. This assumption may apply to engineered *in vitro* preparations better than to *in vivo* preparations, and may apply better during acute ischemia—when there has not been enough time for the collagen matrix to change significantly—than during chronic ischemia. Strains within the heart are large, which implies significant deviations from linearity, but they may not be as large in engineered preparations. In a heart, the ischemic zone will have an irregular geometry that may reach the endocardial or epicardial surface, but in an engineered preparation the experimentalist has more control over the geometry. Thus, the application of a quantitative model of the tissue architecture should be predicated on the validation of the model's assumptions.

Our model allows the computation of strain distributions within uniformly aligned cardiac tissue and represents a design tool for engineered preparations for the study of mechanotransduction signaling pathways in tissues. The model yields an analytical solution for the stress and strain distribution in engineered cardiac tissue and we demonstrate the utility of the model by calculating the strain patterns in and surrounding an ischemic region within the tissue. Such an analytical model demonstrates at a glance how the behavior depends on the parameters of the model and is useful for the design of *in vitro* experiments with engineered tissue preparations. If we were to relax the assumptions of our model, we could not obtain analytical solutions, and we would have to adopt numerical methods. While numerical solutions are valuable, they often do not provide the physical insight that an analytical solution offers. Moreover, our analytical model provides a known solution that others can use to assess the accuracy of their numerical algorithms. Our computationally simple model may be combined with other models of cellular mechanotransduction to predict effects in bulk tissue preparations. For example, the model may

FIG. 2. Distribution of strain parallel to the myocardial fibers in and around a (**a**) circular (two-dimensional) or (**b**) spherical (three-dimensional) inhomogeneity. The tissue outside the inhomogeneity has tension T_o, and the tissue within the inhomogeneity has zero tension. Far from the inhomogeneity, the tissue is fixed. The fiber direction is horizontal. Yellow (positive values) corresponds to stretch of the fibers. The data are calculated taking $a = T_o = \mu = 1$.

FIG. 3. The three-dimensional distribution of strain parallel to the myocardial fibers around a spherical inhomogeneity. The upper surface (y–z) is the same as plotted in Fig. 2b. The fibers lie along the z axis. The strain distribution does not depend on the angle ϕ in the x–y plane. The parameters and color scale are the same as in Fig. 2.

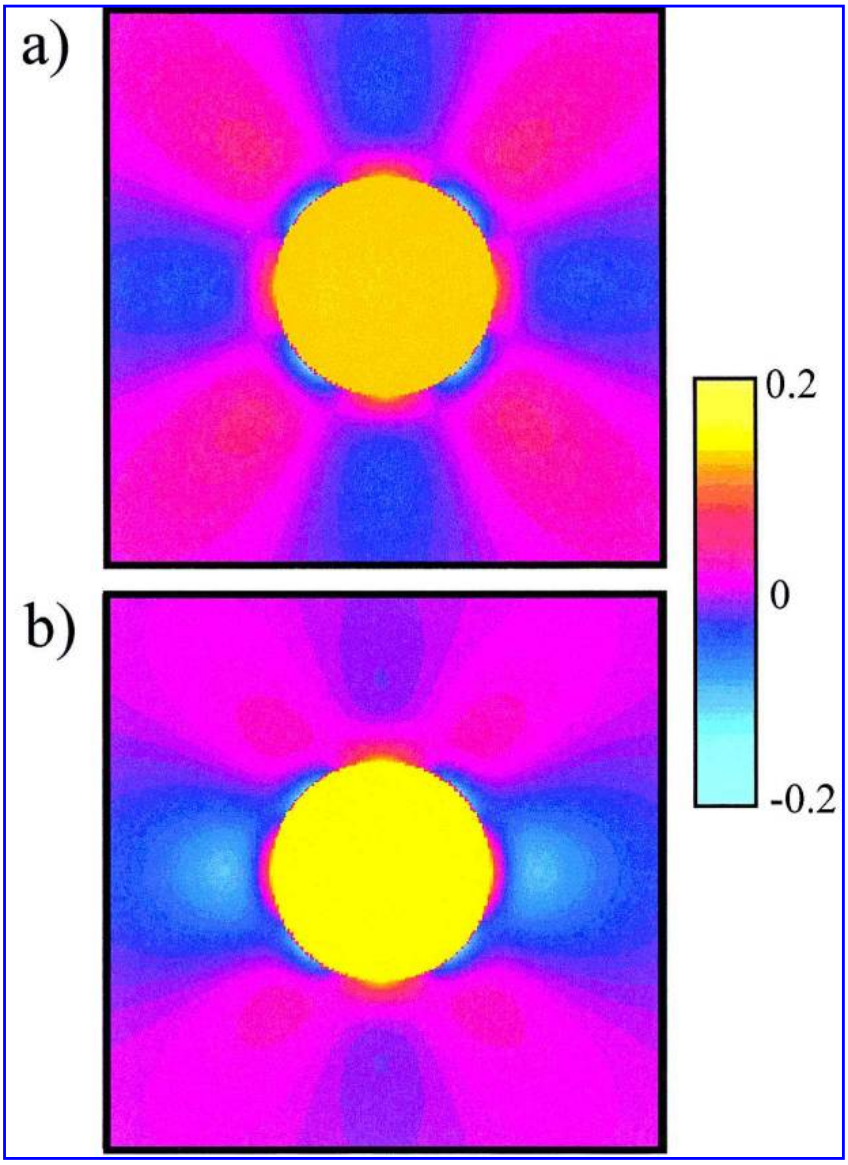

FIG. 2.

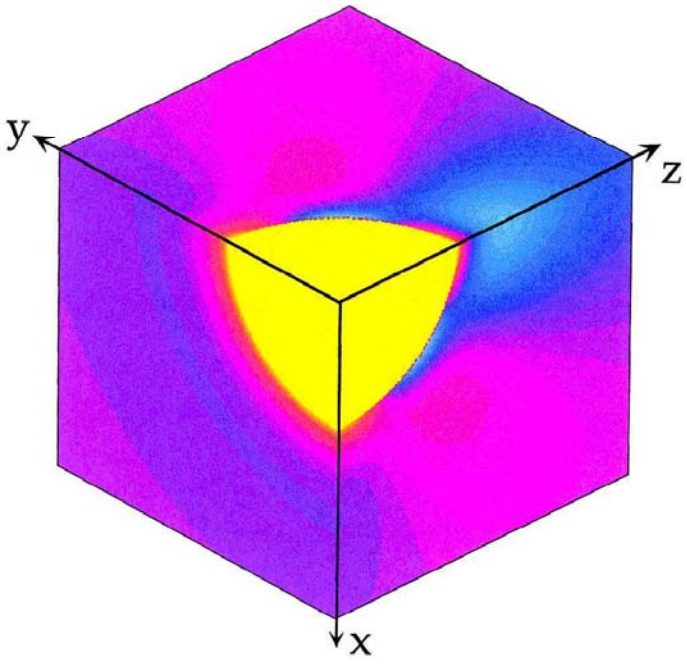

FIG. 3.

be used with models of the heart's electrical activity that take into account stretch-activated channels[24,25] to determine the mechanism of stretch-induced arrhythmias, or to predict fibrosis patterns after stimulated ischemia or hypoxia.

Our model is not the first to examine the mechanical behavior caused by regional ischemia in the heart. Elings *et al.* modeled the isometric tension development in a one-dimensional regionally ischemic muscle.[26] They found that during systole, the ischemic tissue underwent a "paradoxical" stretching. Lew has observed paradoxical stretching during experiments of regional ischemia in dogs.[27] Our Fig. 2 contains a similar finding: the tissue in the inhomogeneous region stretches. Our results extend the Elings *et al.* calculation by predicting the full three-dimensional strain distribution. In particular, we find a complex strain distribution in the normal tissue surrounding the ischemic region that is absent in their one-dimensional model.[26]

Bovendeerd *et al.* measured the strain distribution in a dog with regional ischemia, and also developed a detailed mathematical model of whole-heart mechanical behavior.[28] They concluded that "the deformation pattern of the ventricle was asymmetric with respect to the ischemic region because of the anisotropy of the myocardial tissue." Our model is isotropic and our inhomogeneity was radially symmetric, and thus the deformation pattern was symmetrical about the infarct, but does depend on the direction relative to the fibers. In Fig. 2, the distribution of strain is different in the fiber direction than in other directions. The sign of the strain varies with both angle and radial distance from the ischemic border. Within the border zone, along the fiber direction the tissue stretches next to the border and then shortens farther from the border. Moreover, this behavior appears similar in the directions parallel and perpendicular to the fibers, but of opposite sign at an angle of 45° to the fiber direction. van Leuven *et al.* observed significant gradients of strain across the perfusion boundary during acute myocardial ischemia.[29] Although they do not agree with other researchers regarding the directional differences in the strain distribution, their observation of large strain gradients is consistent with our prediction of significant variations of the strain within the border zone.[30]

ACKNOWLEDGMENTS

This research was supported by the Whitaker Foundation, National Institutes of Health grants R29HL57207 and R01HL58241, and a Predoctoral Fellowship in Cardiology, Institutional Training Grant, NIH 5T32HL07411 (K.K.P.).

REFERENCES

1. Ingber, D.E. Tensegrity: The architectural basis of cellular mechanotransduction. Annu. Rev. Physiol. **59,** 575, 1997.
2. Ko, K.S., and McCulloch, C.A. Intercellular mechanotransduction: Cellular circuits that coordinate tissue responses to mechanical loading. Biochem. Biophys. Res. Commun. **285,** 1077, 2001.
3. Hamill, O.P., and Martinac, B. Molecular basis of mechanotransduction in living cells. Physiol. Rev. **81,** 685, 2001.
4. Schluter, K.D. and Piper, H.M. Regulation of growth in the adult cardiomyocytes. FASEB J. **13**(Suppl.), S17, 1999.
5. Tavi, P., Laine, M., Weckstrom, M., and Ruskoaho, H. Cardiac mechanotransduction: From sensing to disease and treatment. Trends Pharmacol. Sci. **22,** 254, 2001.
6. Taggart, P., and Sutton, P.M. Cardiac mechano-electric feedback in man: Clinical relevance. Prog. Biophys. Mol. Biol. **71,** 139, 1999.
7. Swynghedauw, B. Molecular mechanisms of myocardial remodeling. Physiol. Rev. **79,** 215, 1999.
8. Ruwhof, C., and van der Laarse, A. Mechanical stress-induced cardiac hypertrophy: Mechanisms and signal transduction pathways. Cardiovasc. Res. **47,** 23, 2000.
9. Cohn, J.N. Post-MI remodeling. Clin. Cardiol. **16,** II21, 1993.
10. Whitesides, G.M., Ostuni, E., Takayama, S., Jiang, X., and Ingber, D.E. Soft lithography in biology and biochemistry. Annu. Rev. Biomed. Eng. **3,** 335, 2001.
11. Folch, A., and Toner, M. Microengineering of cellular interactions. Annu. Rev. Biomed. Eng. **2,** 227, 2000.
12. Langer, R., and Vacanti, J.P. Tissue engineering. Science **260,** 920, 1993.
13. Bursac, N., Papadaki, M., Cohen, R.J., Schoen, F.J., Eisenberg, S.R., Carrier, R., Vunjak-Novakovic, G., and Freed, L.E. Cardiac muscle tissue engineering: Toward an in vitro model for electrophysiological studies. Am. J. Physiol. **277,** H433, 1999.
14. Carrier, R.L., Papadaki, M., Rupnick, M., Schoen, F.J., Bursac, N., Langer, R., Freed, L.E., and Vunjak-Novakovic, G. Cardiac tissue engineering: Cell seeding, cultivation parameters, and tissue construct characterization. Biotechnol. Bioeng. **64,** 580, 1999.
15. Papadaki, M., Bursac, N., Langer, R., Merok, J., Vunjak-Novakovic, G., and Freed, L.E. Tissue engineering of functional cardiac muscle: Molecular, structural, and electrophysiological studies. Am. J. Physiol. **280,** H168, 2001.
16. Costa, K.D., Hunter, P.J., Rogers, J.M., Guccione, J.M., Waldman, L.K., and McCulloch, A.D. A three-dimensional finite element method for large elastic deformations of ventricular myocardium. I. Cylindrical and spherical polar coordinates. J. Biomech. Eng. **118,** 452, 1996.
17. Guccione, J.M., Moonly, S.M., Moustakidis, P., Costa, K.D., Moulton, M.J., Ratcliffe, M.B., and Pasque, M.K. Mechanism underlying mechanical dysfunction in the border zone of left ventricular aneurysm: A finite element model study. Ann. Thorac. Surg. **71,** 654, 2001.
18. Ohayon, J., and Chadwick, R.S. Effects of collagen microstructure on the mechanics of the left ventricle. Biophys. J. **54,** 1077, 1988.

19. Love, A.E.H. A Treatise on the Mathematical Theory of Elasticity. New York: Dover, 1944.
20. Aldroubi, A., and Chadwick, R.S. On the uniqueness of quasi-static solutions of some linear models of left ventricular mechanics. Math. Biosci. **99,** 195, 1990.
21. Sachs, F. Modeling mechanical–electrical transduction in the heart. In: Cell Mechanics and Cellular Engineering. New York: Springer-Verlag, 1994, pp. 308–328.
22. Chadwick, R.S. Mechanics of the left ventricle. Biophys. J. **39,** 279, 1982.
23. Chadwick, R.S., Ohayon, J., and Lewkowicz, M. Wall-thickness and midwall-radius variations in ventricular mechanics. Proc. Natl. Acad. Sci. U.S.A. **86,** 2996, 1989.
24. Knudsen, Z., Holden, A.V., and Brindley, J. Qualitative modeling of mechanoelectrical feedback in a ventricular cell. Bull. Math. Biol. **59,** 1155, 1997.
25. Rice, J.J., Winslow, R.L., Dekanski, J., and McVeigh, E. Model studies of the role of mechanosensitive currents in the generation of cardiac arrhythmias. J. Theor. Biol. **190,** 295, 1998.
26. Elings, V.B., Jahn, G.E., and Vogel, J.H.K. A theoretical model of regionally ischemic myocardium. Circ. Res. **41,** 722, 1977.
27. Lew, W.Y.W. Influence of ischemic zone size on non-ischemic area function in the canine left ventricle. Am. J. Physiol. **252,** H990, 1987.
28. Bovendeerd, P.H.M., Arts, T., Delhaas, T., Huyghe, J.M., van Campen, D.H., and Reneman, R.S. Regional wall mechanics in the ischemic left ventricle: Numerical modeling an dog experiments. Am. J. Physiol. **270,** H389, 1996.
29. van Leuven, S.L., Waldman, L.K., McCulloch, A.D., and Covell, J.W. Gradients of epicardial strain across the perfusion boundary during acute myocardial ischemia. Am. J. Physiol. **267,** H2348, 1994.
30. Roth, B.J., and Parker, K.K. Stretch around an inhomogeneity in cardiac tissue. Ann. Biomed. Eng. **26,** S-82, 1998.

Address reprint requests to:
Brad Roth, Ph.D.
Department of Physics
190 Science and Engineering Building
Oakland University
Rochester, MI 48309

E-mail: roth@oakland.edu

This article has been cited by:

1. Marie-Noëlle Giraud , Christine Armbruster , Thierry Carrel , Hendrik T. Tevaearai . 2007. Current State of the Art in Myocardial Tissue Engineering. *Tissue Engineering* **13**:8, 1825-1836. [Abstract] [PDF] [PDF Plus]
2. Phillip Prior, Bradley J. Roth. 2007. Electrostriction of anisotropic tissue. *Physical Review E* **75**:2. . [CrossRef]
3. Marie-Noëlle Giraud, Christime Armbuster, Thierry Carrel, Hendrik T. Tevaearai. 2007. Current State of the Art in Myocardial Tissue Engineering. *Tissue Engineering*, ahead of print070126052142001. [CrossRef]